

# Determination of Ice Age: A Proposed Scheme for a RADARSAT Sea Ice Geophysical Processor System

R. Kwok, D. A. Rothrock<sup>1</sup>, G. F. Cunningham and H. Stern<sup>1</sup>  
Jet Propulsion Laboratory, 4800 Oak Grove Dr, Pasadena, CA 91109  
Tel: (818) 354-5614, FAX: (818) 393-5285  
<sup>1</sup> Polar Science Center, University of Washington, Seattle, WA 98105

## Abstract

We propose a Lagrangian ice motion tracker to follow the trajectory of ice particles at initially fixed grid points in the winter Arctic. From the displacement data, we can derive the area changes associated with a grid cell which we define as the area enclosed by straight line segments connecting four grid points. Any new area created during the time interval between SAR observations contains new sea ice with an age uncertainty equivalent to that of the time interval. During the next time step, the age of this ice is incremented by the size of the time step. A decrease in area is accounted for by ridging the youngest ice. An ice age histogram for accounting for the changes in area is constructed from a series of ice motion observations. A scheme for extended temporal observation of the sea ice cover is proposed. This age distribution can be converted into ice thickness if appropriate environmental conditions are available. We propose that this scheme be implemented in the sea ice geophysical processor system for monitoring of ice age and thickness using RADARSAT data.

## 1. Introduction

The present ER - 1 (geophysical Processor System (GPS)) at the Alaska SAR Facility generates two sea ice products: ice motion [Kwok *et al.*, 1990] and ice type [Kwok *et al.*, 1992]. The GPS ice motion tracker uses a combination of cross-correlation and feature tracking techniques for locating tiepoints in successive SAR image data and has been quite successful in routinely producing a large number of products. The winter ice type classifier categorizes each SAR pixel into one of four ice types: multi-year ice (MY); first-year (FY) deformed; FY smooth; and, a low backscatter type which is characteristic of smooth, younger ice types and calm open water. To date, it has been demonstrated that the MY backscatter is remarkably stable throughout the winter [Kwok *et al.*, 1994] and that fairly accurate observations of the winter MY ice fraction [Fetterer *et al.*, 1994] can be obtained using a simple classification scheme as was implemented in the GPS. Both these products are available from the ASF data archive.

The wide-swath SCANSAR mode of RADARSAT [Raney *et al.*, 1991], to be launched in March 1995, will have the capability to image the Arctic sea ice cover every three days. The ASF science plan for RADARSAT calls for complete coverage of the Arctic

Ocean every 7 days, primarily using this mode. With the available spatial and temporal coverage from RADARSAT, we propose to produce basin-scale fields of geophysical variables with algorithms implemented in a RADARSAT Geophysical Processor System (RGPS). Here, we describe a procedure that provides continual estimates of local ice age and thickness distribution of the Arctic sea ice cover. This procedure is based on our experience with the performance of the ice motion and ice classifier in the present GPS.

## 2. Determination of Age Distribution

The procedure involves Lagrangian observation of ice motion and the interpretation of area changes in cell areas defined by the ice motion tiepoints. A more detailed description can be found in [Kwok *et al.*, 1994].

*Lagrangian tracking.* Initially, a regular array of points is defined on the first image of a long time series. The ice features at these points are identified and tracked in each of the subsequent images thereby providing trajectories of each of these points as a function of time.

*Cell Area and Area Changes.* The array of points in the initial grid constitute the corners of an array of square cells, say, five kilometers on a side. These initial square cells change area and shape as the ice cover deforms. We construct the deformed cells using the trajectory data obtained from the Lagrangian tracker. Any positive change in area indicates that ice in a new age class was formed in that cell between the time of observation. Thus, the resolution of the age of this new age class is dependent on the length of the interval between observations. Any negative area change is assumed to be caused by ridging of the youngest ice in that cell during that same time. Figure 1 shows the deformation of an initial square cell in a time sequence of five SAR images spanning a period of 12 days. The interval between images in the sequence is three days.

*Age Distribution from Time Sequences of Area Changes.* The ice in each cell ages as it progresses through time. If new area is added, a new age category is created. For a negative area change, area is subtracted from the youngest ice categories. The area of ice in each age class is updated in each step of a time series. In this manner, we keep track of the age distribution of ice in the thin end of the distribution. The example in Section 3 illustrates the procedure.

*Conversion to Ice Thickness.* Given the ice age distribution we can convert the ice age to ice thickness with an adequate description of environmental conditions. In the following example, we use a relationships between the thickness of young sea ice and the cumulative number of freezing-degree days (after Maykut, 1986). We used Lebedev's (1938) parameterization, with  $h(\text{thickness}) = 1.33 FDD^{0.58}$ , where FDD = freezing-degree days.

### 3. An Example

We are assuming, in the following example, that the initial distribution contains only FY and MY in the cells. Table 1 shows a record of the parameters recorded at each time step. The MY ice area is obtained using the GPS ice type classification algorithm. The increase in cell area, between Day 077 and Day 086, due to the continual opening of a lead, is evident. The area changes of the cell (in Fig. 1) as a function of time are plotted in Figure 2. This cell had an initial area of 2500 units, 1336 of which were classified as multiyear ice. Over the first time interval (Day 077 to Day 080), the area increased to 3034, giving a young ice class (which is between 0 and 3 days old) an area of 531 units. The remaining 116-I units were assigned to the first-year ice class of undetermined age. The cell area increased to 3205 and 3317 during the second (Day 080 to Day 083) and third (Day 083 to Day 086) time intervals, respectively. This new area of 171 units created during the second time interval replaces the 534 units as the youngest age group. Similarly, the 112 units created during the third time interval replaces the 171 units as having the youngest age. The 534 units created during the first time interval have become 3-6 days and 6-9 days old during the second and third time intervals, respectively, and represent an aging of the ice. A closing event (between Day 086 and Day 089) caused a decrease in cell area from 3317 to 3235, or 82 units. At this time step, the newest age class has zero area since no new area was created, and the next youngest class loses 82 units to account for the lost cell area. 1265 units were classified as MY ice, leaving 1235 units of old FY ice. Note that the area of MY ice does not remain constant throughout the 12-day period. This is due to the high backscatter of the open lead, the signature of which overlaps with that of the MY ice backscatter, leading to an overestimation of MY ice. The time series MY area can be used to determine the correct MY area within the cell area assuming that the MY fraction is invariant within a cell, but we will not discuss this here. Figure 3 shows the estimated ice thickness using the simple parameterization discussed above.

### 4. Summary Remarks

We have provided a brief description of a procedure for monitoring the local age distribution of sea ice using a long sequence of ice motion observations. The application of this procedure is restricted to winter Arctic conditions because of the assumption of ice growth in open leads. In the general scheme, we suggest starting the process during fall freeze-up and continuing for the whole seasonal cycle through the onset of melt to obtain a record of the age distribution for the Arctic ocean. At each time step, we would determine the ice age through a procedure which includes ice motion tracking, computation of area changes and the update of the local ice age histogram. Regional scale statistics of ice age or thickness are estimated from the local observations.

The RADARSAT SAR, which will be launched in January 1995, will have the capability to image the ice cover every three days. This scheme could be implemented in a new Geophysical Processor System to provide Arctic-wide fields of motion and age distributions.

### Acknowledgments

R. Kwok and G. F. Cunningham performed this work at the Jet Propulsion Laboratory, California Institute of Technology under contract with the National Aeronautics and Space Administration. D. A. Rothrock and J. L. Stern performed this work at the Applied Physics Laboratory, University of Washington under NASA contract, NAGW-2513.

### References

- Fetterer, F., D. Gineris and R. Kwok, An Assessment of Arctic Multi-year Ice Coverage Estimated Through Alaska SAI Facility Data Analysis, Submitted to *JGR-Oceans*.
- Kwok, R., J. C. Curlander, R. McConnell and S. Pang, An Ice Motion Tracking System at the Alaska SAR Facility, *IEEE J. of Oceanic Engineering*, Vol. 15, No. 1, 44-54, 1990.
- Kwok, R., E. Rignot, B. Holt and R. G. Onstott, Identification of Sea Ice Types in Spaceborne SAR Data, *J. Geophys. Res.*, 97 (C2), 2391-2402, 1992.
- Kwok, R. and G. Cunningham, Backscatter Characteristics of The Sea Ice Cover in the Winter Beaufort Sea, to be published in *JGR-Oceans*.
- Kwok, R., D. A. Rothrock, H. Stern and G. F. Cunningham, Determination of The Age Distribution of Sea Ice from Lagrangian Observations of Ice Motion, Submitted to *IEEE Trans. Geo. and Rem. Sens.*.
- Maykut, G. A., The Surface Heat and Mass Balance, in *Geophysics of Sea Ice*, Ed. N. Untersteiner, Series B: Physics [101, 146, 1986.
- Raney, R. K., A. P. Luscombe, E. J. Langham and S. Ahmed, RADARSAT, *Proceedings of the IEEE*, Vol. 79, No. 6, June, 1991.

Table 1

Record of Parameters (Area changes, Age Distribution) from Tinw-sequence Analysis  
(Example 1)

Record	Time (DAY:HH)	Mean Temp, $T$	Cell Area, $A$	FDD	Area* of Age Class $j$					
					1	2	3	4	FY	MY
1	077:22	-23	2500						1164	1336
2	080:22	-20	3034	65	534				598	1902
3	083:22	-20	3205	126	171	534			536	1964
4	086:22	-19	3317	166	112	171	534		1046	1454
5	089:22	-17	3235	229	0	30	171	534	1235	1265

\* 1 pixel = 100m  $\times$  100m = 10000  $m^2$  = unit area  
FDD = Cumulative freezing-degree days



Figure 1. An image sequence showing the deformation of a grid cell. The time interval between the images is 3 days. (SAR images: Copyright ESA 1993).

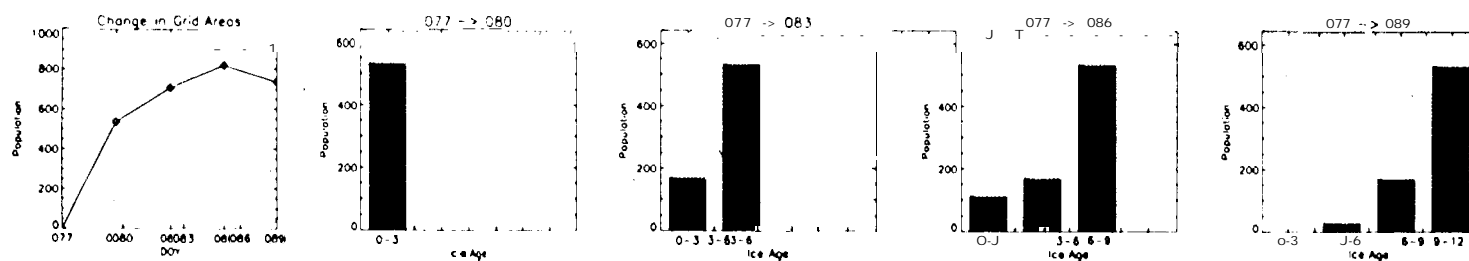


Figure 2. Determination of ice age distribution within the grid cell in Fig. 1. Plot of area changes as a function of time, and age histograms computed from the area changes. (1 pixel = 100m  $\times$  100m = 10000  $m^2$  = unit area)

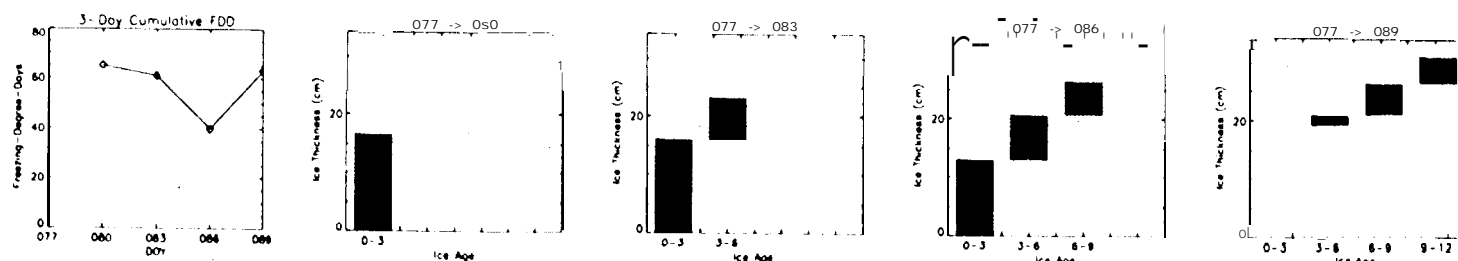


Figure 3. Determination of ice thickness distribution. Plot of the freezing-degree days and the computed thickness of the ice.